International Journal of Energy and Water Resources (2019) 3:141–152
https://doi.org/10.1007/s42108-019-00024-w

ORIGINAL ARTICLE

Application of sugarcane leaves as biomass in the removal of cadmium(II), lead(II) and zinc(II) ions from polluted water

O. A. Adigun[1,2] · V. O. Oninla[3] · N. A. Adesola Babarinde[4]

Received: 20 February 2019 / Accepted: 7 May 2019 / Published online: 22 May 2019

Abstract

Here, we present the removal of cadmium(II), lead(II) and zinc(II) ions, by sugarcane (*Saccharum spontaneum*) leaves. Biomass characterisation was performed with Fourier transform infrared spectroscopy, scanning electron microscopy, energy dispersive X-ray and X-ray diffractometry. The effects of parameters such as solution pH, initial metal ion concentration and contact time were investigated. To understand the adsorption process, data were fitted into models such as the pseudo-first order, pseudo-second order, Weber–Morris, Langmuir, Freundlich and Dubinin–Radushkevich (D–R). The surface of the adsorbent was oval and irregular in shape, with scattered adsorptive sites. Carbon and oxygen were the main element present in the adsorbent, claiming about 59% and 38% of the total elemental compositions, respectively. Optimum pH for lead and zinc ions was 5, while 6 was chosen for cadmium ions. Adsorption increased with time and eventually plateaued after 5 h for lead and 4 h for cadmium and zinc ions. Metal uptake increased with increase in initial metal ion concentration up to 250 mg/L. Adsorption data fitted best to the Langmuir isotherm, with maximum sorption capacity, q_{max}, obtained as 142.86, 156.25 and 166.67 mg/g for the removal of cadmium, lead and zinc, respectively. The pseudo-second-order model provided the best fit for the kinetic data (R^2 of > 0.95), indicating that the sorption process was controlled by chemisorption mechanism. Information from Freundlich and D–R models signified that the uptake of the three metal ions was by physisorption and that ion-exchange mechanism was also involved in zinc adsorption.

Keywords Adsorption process · Isotherm · Kinetic mechanism · Metal uptake · Physisorption

Introduction

The discharge of untreated industrial effluents and sewage from metabolic wastes into water bodies, especially in the developing countries, has been on the increase for some years. Due to the debilitating effects of this environmental pollution on the ecosystem (Gnanasekaran et al. 2015), global environmentalists have since been looking for ways of combating the menace. One of the main reasons for the upsurge is the steady increase in the urbanisation and industrialisation trend around the world, which results in large pollutants being released into the environment (Denny 1997; Muñoz et al. 2018). Other reasons include high cost of advanced technological methods for the treatment of wastewater and insufficient information on the danger the pollutants pose to aquatic and human lives (Denny 1997; Krishnani et al. 2008).

Heavy metal ions are regarded as environmental toxins and elevated concentrations of these toxic metal ions have been detected in some rural areas of the world (Denny 1997). Cadmium(II), lead(II) and zinc(II) are few of the toxic metal ions that pollute natural potable water sources. These hazardous metal ions and other pollutants are released into the environment via indiscriminate discharge of toxic chemicals through effluents from a wide

✉ O. A. Adigun
oaadigun@mun.ca

✉ V. O. Oninla
vinzoninla@daad-alumni.de

1 Department of Chemistry, University of Ibadan, Ibadan, Nigeria

2 School of Science and the Environment/Boreal Ecosystem Research Facility, Memorial University of Newfoundland, Grenfell Campus, 20 University Drive, Corner Brook, NL A2H 5G4, Canada

3 Department of Chemistry, Obafemi Awolowo University, Ile-Ife, Nigeria

4 Department of Chemical Sciences, Olabisi Onabanjo University, Ago-Iwoye, Nigeria

range of industries. Industrial units such as steel, oil, canneries, refineries, mines and electroplating units are the major culprits of heavy metal pollution in the environment (Reddy et al. 2011; Albadarin et al. 2012). Dreadful human illnesses such as disruption of protein metabolism, induced sterility, neonatal death, calcium substitution in bones, hypertension, cancerous growth and accumulation in food chain have been traced to toxic metal ion intake (Naushad et al. 2016). Since these toxic metal ions are non-biodegradable, once released into the environment, they remain and some eventually find their ways into living system where they accumulate (Cazón et al. 2013).

The fact that toxic metal ions stay in the environment or accumulate in living system with their attendant ill-effects has led to global concerted effort aimed at remedying the environment by preventing large concentrations of these toxins from getting into the water body. In treating industrial wastewaters, a number of conventional techniques such as ion-exchange, precipitation, reverse osmosis, solvent extraction, solid phase extraction, evaporation, membrane filtration and adsorption have been employed (Muñoz et al. 2018). Of all these techniques, adsorption has gained widespread popularity, mainly due to the advantages it has over all other techniques, which include its relative simplicity, low cost, high efficiency, minimisation of biological sludge, regeneration of adsorbent and possibility of effluent recovery (Pino et al. 2006).

The passive sorption and complexation of metals and other toxins from polluted water by non-viable biomass (i.e. dead biomass), which could be of plant origin or animal derived materials, is referred to as biosorption (Krishnani et al. 2008; Cazón et al. 2013). A number of adsorbents have been tested for their metal uptake capacities. They include: cassava tuber bark (Horsfall et al. 2006), coconut shell powder (Pino et al. 2006), rubber leaf powder (Kamal et al. 2010) and rice husk (Muñoz et al. 2018).

Sugarcane leaves are generally regarded as waste and they are readily available in abundance, especially in large-scale sugarcane plantations. The present study was therefore aimed at characterising and evaluating the adsorption capacity of sugarcane leaves (SCL) in the removal of Cd^{2+}, Pb^{2+} and Zn^{2+} from aqueous solution in a batch experimental process. The effects of different parameters such as pH, contact time and initial metal ion concentration were investigated. Moreover, adsorption data were fitted to different models to determine the kinetics and the isothermal behaviour of the sorption process. The greater part of the research work was carried out at the University of Ibadan, Nigeria; while the concluding part was undertaken at the Obafemi Awolowo University, Ile-Ife, Nigeria, in 2019 and partly characterised in South Africa.

Materials and methods

Preparation of SCL biosorbent

Sugarcane leaves were obtained from a sugarcane plantation in Mamu village in Ijebu-Igbo, Ijebu South Local Government Area of Ogun State, South West, Nigeria. The leaves were thoroughly rinsed with water from a tap and then with deionised water. The washed leaves were air-dried for about 2 weeks and later oven dried for 5 h at 70 °C. The dried leaves were pulverised. Further drying was carried out at 50 °C for 6 h. The pulverised leaves, thenceforth referred to as SCL, was sieved through a 420 µm mesh and stored in an airtight plastic container for further use.

Preparation of metal ion solution

All chemicals used in this study were obtained from Sigma-Aldrich and were used without further purification. Standard solutions of Cd^{2+}, Pb^{2+} and Zn^{2+} used for the study were prepared by dissolving appropriately weighed amount of $Cd(NO_3)_2.4H_2O$, $Pb(NO_3)_2$ and $ZnSO_4{\cdot}7H_2O$, respectively, in a 1000 mL standard flask and made up to the mark with deionised water. The concentration of the stock solution of each metal ion was 1000 mg/L, out of which fresh dilutions were made as required. Standardisation of the bulk solution was carried out by atomic absorption spectrophotometer (Buck-Scientific 210 VGP) with deuterium background correlator.

Surface characterisation of SCL

Characterisation of the SCL was performed with Fourier transform infrared spectroscopy (FTIR), scanning electron microscopy (SEM), energy dispersive X-ray (EDX) and X-ray diffractometry (XRD). The FTIR analyses of the unloaded and toxic metals-loaded SCL were carried out with Shimadzu FTIR-8400S Spectrometer (at the scanning frequencies of 400–4000 cm^{-1}). SEM micrographs and EDX spectra of unloaded and metal-loaded SCL samples were obtained using a Zeiss Ultra Plus 55field emission scanning electron microscope (FE-SEM) actuated at 1.0 kV. Identification of the diffraction pattern of SCL was done using Rigaku Ultima IV X-Ray Diffractometer (XRD). The sample was gently consolidated in a copper holder and scanned at 40 mV/40 mA, scan speed = 1.000 deg/min; the scan mode was continuous and scan range was between 5000° and 100,000°.

Proximate analysis (PA) and bulk density (BD) of SCL

Proximate analysis of SCL was carried out according to the procedure of Official Analytical Chemist (AOAC 1990). Bulk density was determined according to the protocol of

Table 1 Kinetic and equilibrium models used in this study

Model	Integrated equation	References
Kinetic models		
Pseudo-first order	$\ln(q_e - q_t) = \ln q_e - k_1 t$	Lagergren (1898)
Pseudo-second order	$\frac{t}{q_t} = \frac{t}{q_e} - \frac{1}{k_2 q_e^2}$	Ho and McKay (1999)
Weber–Morris	$q_t = k_\alpha t^{1/2} + C$	Weber and Morris (1963)
Equilibrium models		
Langmuir	$\frac{1}{q_e} = \left(\frac{1}{q_{max} K_L}\right)\frac{1}{C_e} + \frac{1}{q_{max}}$	Langmuir (1918)
Freundlich	$\ln q_e = \ln K_f + \frac{1}{n} \ln C_e$	Freundlich (1906)
Dubinin–Radushkevich	$\ln q_e = \ln q_m - \beta\varepsilon^2$ $\varepsilon = RT \ln\left(1 + \frac{1}{C_e}\right)$	Dubinin et al. (1947)

Ofomaja and Naidoo (2011). Briefly, a 25 cm^3 density bottle was weighed empty and then filled with the SCL with 'gentle tapping' to ensure proper filling and elimination of air spaces. After filling, the density bottle was weighed with its content. The difference between the final and initial weights of the bottle gave the mass of the biosorbent that occupied 25 cm^3 density bottles.

Biosorption studies

Metal uptake capability of SCL was studied by varying the solution pH, contact time and the initial metal ion concentration (one at a time) in a batch adsorption process. With the exception of concentration dependence study, where the initial metal ion concentration was varied, all studies were performed by contacting 0.1 g of SCL with 50 mL of 100 mg/L Cd^{2+}, Pb^{2+} and Zn^{2+} ion solutions in corked 125 mL Pyrex Erlenmeyer flasks. Equilibration was performed at 200 rpm in a thermostatic water bath and shaker (Haake Wia model) and the experimental temperature was set at 27 °C. Each study was performed in duplicate with the average of the two values taken. The effect of pH on the biosorption of metal ions was carried out within the pH range of 2–7. Adjustment of pH was performed by dropwise addition of either HNO_3 or NaOH. The mixtures were agitated for 2 h. The effect of contact time was studied at various agitation times (0–400 min), with the solution pH adjusted to the optimum value for each metal ion. The effect of initial metal ion concentration was studied by varying the adsorbate concentration from 10 to 500 mg/L. Contact time and pH were set at the optimum condition determined earlier for each metal ion. After agitation, the metal-laden biosorbent was recovered by filtration, using Whatman's #42 filter papers. The filtrate was afterwards analysed by atomic absorption spectroscopy for residual metal ions. The metal uptake capacity of SCL, expressed as percentage of metal ions adsorbed or milligrams of biosorbed ions per gram of dry mass of the biomass, q_e, was determined by the following equations:

$$\% \text{ adsorbed} = \frac{(C_o - C_e)}{C_o} 100, \tag{1}$$

$$q_e = \frac{(C_o - C_e)V}{m}, \tag{2}$$

where C_o, C_e, m and V are the initial metal ion concentration (mg/L), equilibrium metal ion concentration (mg/L), mass of the biosorbent (g) and volume of the solution (L), respectively.

Experimental data were fitted into different kinetic and equilibrium models to determine the best models that describe the adsorption process. The models considered are the pseudo-first-order (Lagergren 1898), pseudo-second-order (Ho and McKay 1999), Weber–Morris intra-particle diffusion (Weber and Morris 1963), Langmuir (Langmuir 1918), Freundlich (Freundlich 1906) and Dubinin–Radushkevich (Dubinin et al. 1947) models. The linearised forms of these models are as shown in Table 1.

Results and discussion

Surface characterisation of SCL

FTIR study of SCL

Metal uptake capacity of an adsorbent is dependent on the chemical reactivity of functional groups present at the adsorbent surface as well as its surface porosity. Figure 1 shows the FTIR spectra of unloaded and metal-loaded SCL. The FTIR spectrum of unloaded SCL reveals a number of characteristic absorption bands. The broad band at 3448 cm^{-1} has been assigned to the surface O–H/N–H stretching vibration and weakly absorbed water (Zhou et al. 2015). The peaks at 2918 cm^{-1} and 2850 cm^{-1} were attributed to symmetric and asymmetric C–H stretching. The bands at 1726 cm^{-1} and 1633 cm^{-1} have been assigned

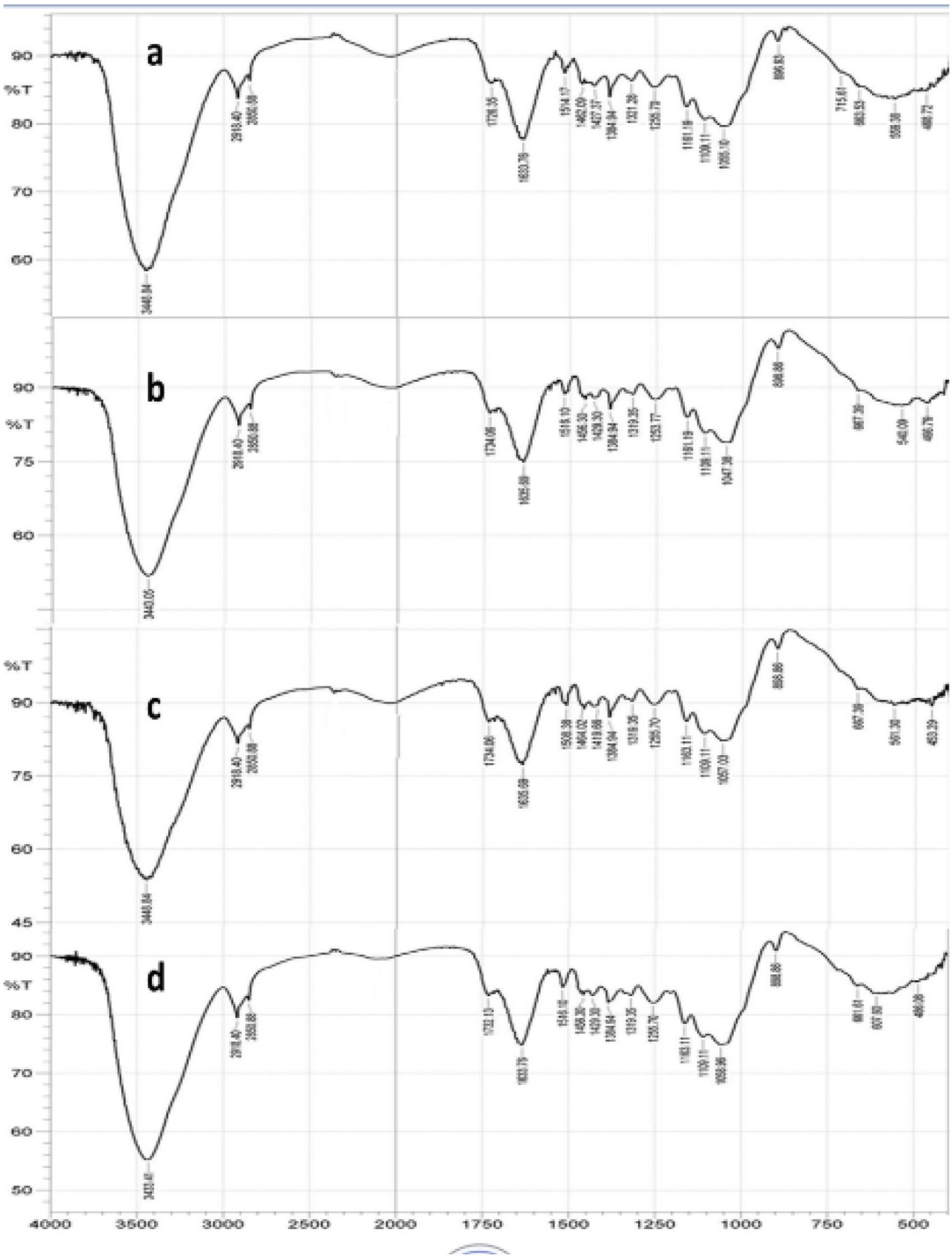

Fig. 1 FTIR spectra of unloaded and metal-loaded SCL. Spectra a, b, c and d represent unloaded, Cd-loaded, Pb-loaded and Zn-loaded SCL, respectively

to the C=O stretching vibration. Peaks at 1462–1380 cm^{-1} could be due to alkyl C–H bend, aromatic C=C stretch and C–O stretch (Babalola et al. 2016). Other peaks observed at 1514, 1255 and 1055 cm^{-1} were assigned to aromatic stretching rings from lignin, C–O linkage/OH in-plane bending in cellulose (Castro et al. 2017) and C–O stretch, respectively. As shown in Fig. 1b–d, after the uptake of the various metal ions, the absorption band at 3448 cm^{-1} shifted to 3443 cm^{-1} and 3433 cm^{-1} in the spectra of Cd- and Zn-loaded SCL, respectively,

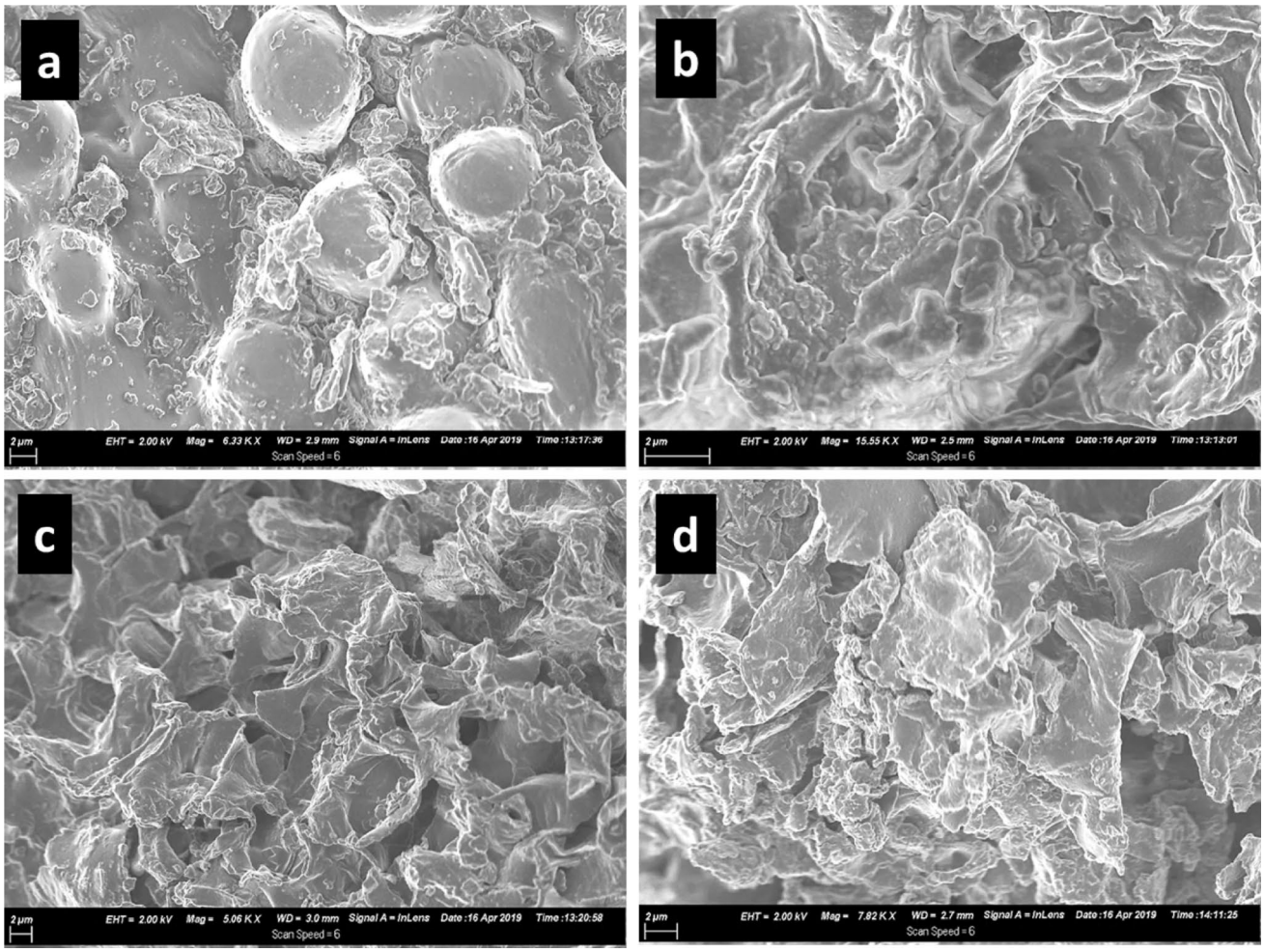

Fig. 2 SEM micrographs of **a** unloaded, **b** Cd-loaded, **c** Pb-loaded and **d** Zn-loaded SCL

suggesting the involvement of the O–H functional group in the metal removal process. That same peak, however, remained unchanged in the spectrum of Pb-loaded SCL, possibly indicating a weak interaction. Comparison of the four spectra indicates a shift in the band at 1726 cm^{-1}, in the spectrum of unloaded sample, to 1734 cm^{-1} after the adsorption of Cd^{2+} and Pb^{2+}, and 1732 cm^{-1} after the adsorption of Zn^{2+}. Displacement was also observed in the C=O band at 1633 cm^{-1} as well as in the peaks representing C–O stretching vibration, indicating the possible utilisation of the carbonyl and carboxyl functional groups, along with the hydroxyl, in the metal-binding process.

Scanning electron microscopy (SEM) EDX and XRD analyses

The surface morphologies of SCL (before and after metal adsorption) were examined by scanning electron microscopy (SEM). The SEM micrographs of unloaded and metal-loaded SCL are shown in Fig. 2. The images, taken at high magnifications, reveal that the particles of unloaded SCL (Fig. 2a) were oval and irregular in shape (Qin et al. 2016) with scattered pores observed all through its surface. The abundance of these pores suggests the potentials of SCL in efficiently adsorbing toxic materials. After the uptake of the various metal ions, the surface morphology of the adsorbent changed—the disappearance of the oval shape was observed (Fig. 2b–d). Figure 3 shows the EDX spectra of SCL before (a) and after adsorption of metal ions (b–d). As indicated by the spectrum of unloaded sample (Fig. 2a), SCL is mainly made up of carbon (C) and oxygen (O), comprising about 59% and 38% of the total constituent elements, respectively. No Cd, Pb and Zn were observed. However, as shown in Fig. 3b–d, the spectra of the adsorbent after adsorption show prominent peaks of the respective metals involved, thereby indicating that adsorption of the metals actually took place. X-ray diffraction was performed to determine the crystalline structure of SCL. The XRD pattern, shown in Fig. 4, indicates some peaks—one intense peak and other secondary peaks. The main and intense peak at θ of 23° reveal the presence of highly organised crystalline cellulose, while

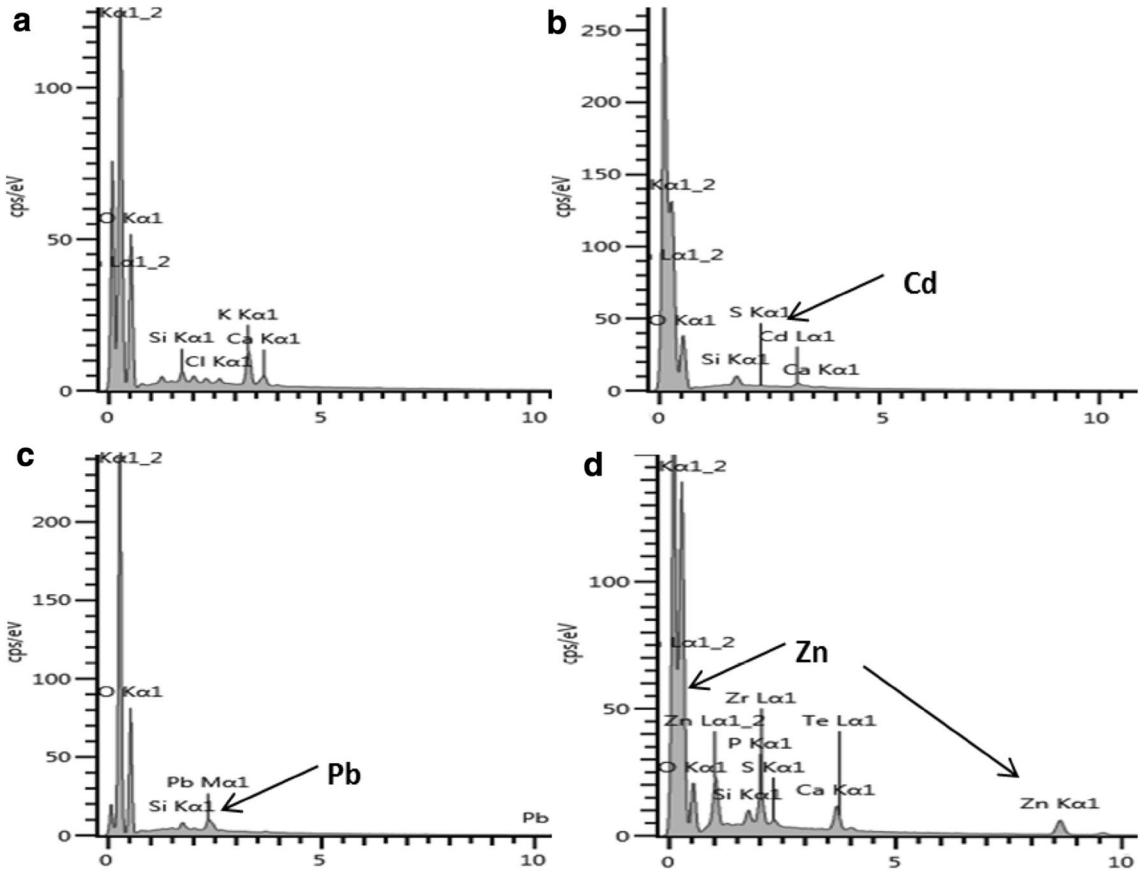

Fig. 3 EDX spectra of **a** unloaded, **b** Cd-loaded, **c** Pb-loaded and **d** Zn-loaded SCL

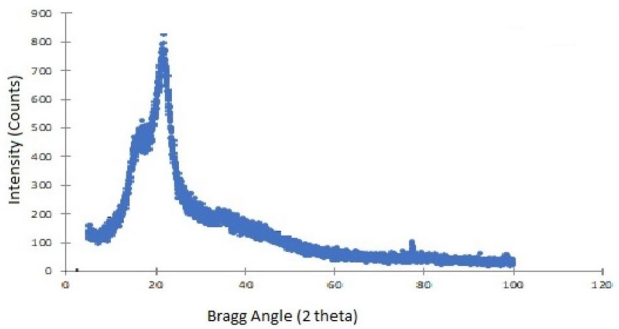

Fig. 4 XRD pattern of SCL

the other weak secondary peak, especially the one at θ of 17°, characterises less organised functional moieties such as polysaccharides and lignin present in SCL (Zhou et al. 2015; Babalola et al. 2016).

Proximate analysis (PA) and bulk density (BD)

Proximate analysis of SCL showed that the biosorbent contained 6.34, 12.22, 25.41, 1.33 and 34.20% of moisture content, ash content, crude fibre, crude protein and starch content, respectively. The presence of high crude fibre and starch content indicates that SCL contains lignocellulose and hemicellulose moieties required for effective adsorption of toxic pollutants. The measured bulk density of the biosorbent is 0.34 g/mL. Bulk density evaluates the quality of adsorbents—low bulk density is an indication of high porosity, leading to high adsorption capacities on a weight basis (Liu et al. 2018). Therefore, the low bulk density of SCL signifies that the adsorbent has the capacity to hold more metal ions per unit volume.

Batch biosorption of Cd^{2+}, Pb^{2+} and Zn^{2+} ions by SCL

Influence of pH

This study attests to the significant role solution pH plays in the adsorption process. The phenomenon of adsorption of solute ions onto the active sites of biosorbents is greatly influenced by solution pH. This is due to the possibility of protons being adsorbed or released from the adsorbent surface (Jin et al. 2018). The solution pH regulates the solubility as well as the speciation of the adsorbate ions in solution. It

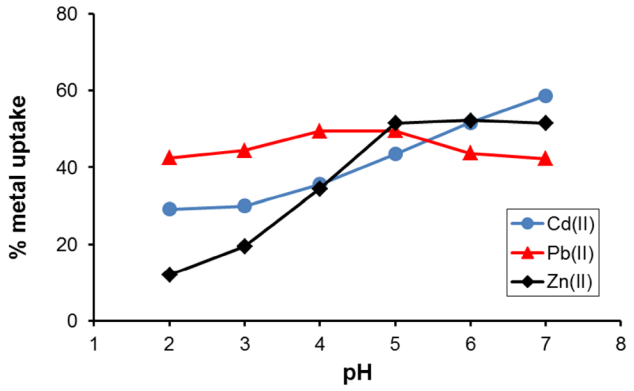

Fig. 5 Effect of pH on the biosorption of Cd^{2+}, Pb^{2+} and Zn^{2+} by SCL (SCL dose: 100 mg; agitation time: 2 h; initial metal concentration: 100 mg/L; temperature: 27 °C)

also determines the surface charge of the adsorbent (Oninla et al. 2018). As shown in Fig. 5, % metal uptake for each of the three metals under study was obtained at different values at different solution pH values. Adsorption of Cd^{2+} was observed to increase with rise in solution pH from 2 to 7, while those of Pb^{2+} and Zn^{2+} ions increased from pH 2 to 5. Whereas % Pb^{2+} uptake decreased, no significant Zn^{2+} uptake was noticed with further rise in solution pH. At the pH of optimum adsorption, 58.6, 49.5 and 52.2% uptakes of Cd^{2+}, Pb^{2+} and Zn^{2+} ions, respectively, were observed. The low metal uptake observed at highly acidic pH could be as a result of electrostatic repulsion to the metal cations and the protonation of the binding sites on the surface of the SCL, occasioned by high abundance of hydrogen ion (Huptake up to pH 7, and possibly beyond, might) in the medium (Jin et al. 2018). However, with continuous rise in pH, the metal ions gained advantage because the carboxyl and hydroxyl functional groups on the SCL surface became deprotonated, thereby increasing the density of negative charge ions on the adsorbent surface, which in turn tremendously enhanced the electrostatic attraction between the metals and the SCL (Oninla et al. 2018). The continuous rise in Cd^{2+} uptake up to pH 7, and possibly beyond, might, nonetheless, not be solely due to pH influence: other factors such as adsorption of hydrolysis products and precipitation of colloidal slightly soluble or insoluble metal hydroxides at high pH could as well contributed to the phenomenon observed (Vijayaraghavan et al. 2017). Thus, to eliminate other influences as much as possible, the pH of Cd^{2+} solution was set at 6. A similar trend has also been reported for the adsorption of Cd^{2+} by immobilised *Pleurotus ostreatus* spent substrate (Jin et al. 2018). The seemingly constant values of Zn^{2+} uptake from pH 4 could be due to adsorption/desorption equilibrium, indicating no significant influence of pH on Zn^{2+} adsorption onto the SCL biosorbent from pH 5 to 7.

Influence of contact of time

In designing cost-effective systems for wastewater treatment, equilibrium contact time is one major factor often considered (Hassoune et al. 2018). Time dependence study is very vital, as it provides kinetic data for the prediction of adsorption rate, the information which is of great relevance in the design of full-scale adsorption process (Vijayaraghavan et al. 2017). Information obtained from the effects of the duration of contact of SCL with the solutions of Cd^{2+}, Pb^{2+} and Zn^{2+} ions (Fig. 6a) indicates that most biosorption of Cd^{2+} and Zn^{2+} took place within the first 3 and 4 h, respectively; and that a contact time of 4 h was sufficient to attain adsorption/desorption equilibrium. On the other hand, biosorption of Pb^{2+} increased with rise in contact period and possibly reached equilibrium between 5 and 6 h. Within the first 5 min of contact between the SCL and the adsorbates, 29.46, 23.48 and 25.8 mg/g of Cd^{2+}, Pb^{2+} and Zn^{2+}, respectively, were removed, indicating the exposure of a large number of binding sites on the SCL, which caused rapid metal binding at the earlier stage of the sorption process. It could also be because of the high concentration gradient, which enhanced the mass migration of the metal ions from the bulk phase to the surface of the SCL and the consequent rapid binding to the functional groups present at the active sites of the adsorbent.

As the adsorbent stayed longer in the solution, the rate of Zn^{2+} and Pb^{2+} uptake slowed until attainment of equilibrium, although Cd^{2+} sorption gained a little momentum after 100 min prior to equilibrium state. A relatively more pronounced increase in uptake was observed in case of Cd^{2+} uptake by SCL between 5 min and 1 h, after which the uptake rate slowed. The slow uptake after the initial sharp rise suggests the occupation of a vast number of the SCL active sites within the first 5 min, making the remaining yet unoccupied sites less accessible, probably due to repulsive forces between the already adsorbed metal ions and the bulk phase.

Influence of initial metal ion concentration

The dependence of the adsorption of Cd^{2+}, Pb^{2+} and Zn^{2+} ions on the initial concentrations of the metals is depicted in Fig. 6b. The study was carried out at different initial metal ion concentrations ranging from 10 to 500 mg/L. A progressive rise in metal uptake by SCL was observed with increase in metal ions concentration up till 250 mg/L, after which adsorption/desorption equilibrium was attained. At equilibrium, 132.52 mg/g, 146.61 mg/g and 156.12 mg/g of Cd^{2+}, Pb^{2+} and Zn^{2+} ions, respectively, were adsorbed, indicating a better efficiency of SCL in the removal of Zn^{2+} ion, when compared with Cd^{2+} and Pb^{2+} ions. The initial sorbate concentration is an important factor in any adsorption process.

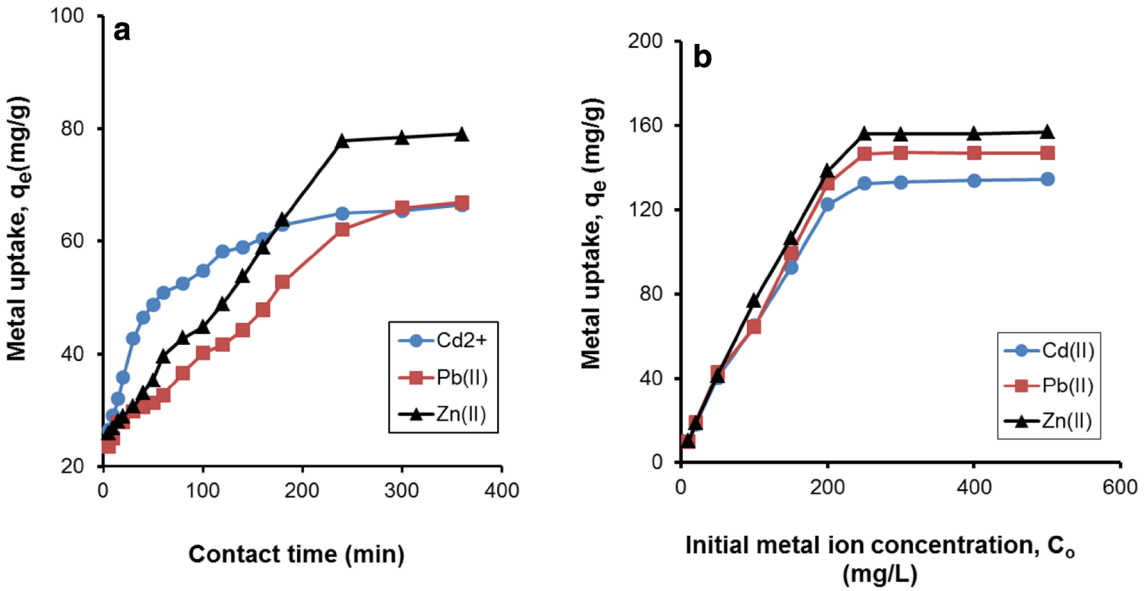

Fig. 6 Effect of **a** contact time and **b** initial metal ion concentration on the biosorption of Cd^{2+}, Pb^{2+} and Zn^{2+} by SCL (SCL dose: 100 mg; agitation time: 5–400 min; initial metal concentration: 10–500 mg/L; temperature: 27 °C)

At low initial metal ion concentration, few metal ions were present in the solution. This consequently resulted in few active sites on the SCL surface being occupied. Increasing the initial metal ion concentrations, however, raised the number of metal ions in the solution, leading to continuous occupation of more active sites on the adsorbent (Oninla et al. 2018). Most researchers have also reported increase in sorbate uptake with increasing initial concentration (Ofomaja and Naidoo 2011; Babalola et al. 2016; Castro et al. 2017). This common phenomenon could most likely be due to increasing driving force needed to overcome all resistances to mass transfer between the solution and the adsorbent as initial concentration increases. Here, increase in the initial concentrations of Cd^{2+}, Pb^{2+} and Zn^{2+} ions in the solution possibly provided the necessary driving force needed to overcome all resistances to mass transfer of the metal ions between the solution and the SCL, thus resulting in increasing likelihood of collision between the metal ions in the solution and the SCL biosorbent (Hassoune et al. 2018).

Modeling of the sorption process

Equilibrium study

To explain the process of the adsorption of Cd^{2+}, Pb^{2+} and Zn^{2+} ions onto the surface of SCL, data from the batch adsorption study were fitted to three different equilibrium isotherm models, namely, Langmuir, Freundlich and Dubinin–Radushkevich (D–R) isotherms. The linearised equations for the various models are shown in Table 1. Here, q_{max} (mg/g) represents maximum adsorption capacity; C_e (mg/L) is equilibrium concentration of metal ion; K_L (L/mg) is Langmuir constant; K_f (mg/g) and n represent Freundlich constant and intensity constant, respectively; R, with the value of 8.314 J/mol K, represents the universal gas constant; T (K) is the temperature; β (mol^2/kJ^2) is the D–R constant; and ε (J/mol) represents Polanyi constant. Parameters for the models, shown in Table 2, were obtained from the linear plots of the models' equations. The parameter, R^2, known as determination coefficient, was adopted to determine the model that best described the adsorption process. R^2 value of 1 is an indication of the perfect description of a sorption process, and the closer the R^2 value of experimental data plot to unity, the better the model is in describing an adsorption process. A critical look at the values of R^2 obtained by fitting the experimental data to the four models showed the Langmuir isotherm (with R^2 value of 0.992, 0.986 and 0.994 for Cd^{2+}, Pb^{2+} and Zn^{2+} ions, respectively) as the best model in describing the adsorption of the three metal ions onto the surface of SCL. This, therefore, signifies monolayer adsorption, implying that the adsorption of the three metals occurred more at specific homogeneous sites on the SCL (Langmuir 1918).

The maximum adsorption capacity, q_{max}, of SCL for the uptake of Cd^{2+}, Pb^{2+} and Zn^{2+} ions was determined as 142.9 mg/g, 156.3 mg/g and 166.7 mg/g, respectively. Although Cd^{2+}, Pb^{2+} and Zn^{2+} are all divalent ions with ionic charge of +2, they possess different ionic radii and sizes (Cotton and Wilkinson 1980), and therefore are expected to be adsorbed on SCL at different q_{max} and rates, in the order of Zn^{2+} (0.69 Å) > Cd^{2+} (1.03) > Pb^{2+} (1.17

Table 2 Kinetic and equilibrium parameters for the biosorption of Cd^{2+}, Pb^{2+} and Zn^{2+} by SCL

	Parameter	Cd^{2+}	Pb^{2+}	Cr^{3+}
Kinetic model				
Pseudo-first order	R^2	0.8667	0.7628	0.8287
	k_1 (L/min)	0.0176	0.0173	0.0195
	q_e (mg/g)	54.174	96.757	130.634
Pseudo- second order	R^2	0.9987	0.9586	0.9583
	k_2 (g/(mg min))	0.0007	0.0003	0.0002
	q_e (mg/g)	69.444	72.993	89.286
Weber–Morris	R^2	0.8711	0.9689	0.9626
	k_α (mg/g $min^{½}$)	2.2430	2.7006	3.5013
	C	28.806	14.784	13.542
Equilibrium isotherm model				
Langmuir	R^2	0.9922	0.9861	0.9942
	k_L (L/mg)	0.0490	0.0580	0.0670
	q_{max} (mg/g)	142.857	156.250	166.667
Freundlich	R^2	0.9664	0.9688	0.9312
	k_F (L/mg)	14.078	20.094	27.270
	$1/n$	0.4334	0.3821	0.3290
Dubinin–Radushkevich (D–R)	R^2	0.8873	0.9560	0.9368
	q_m (mg/g)	0.0355	0.0093	0.0403
	E (kJ/mol)	7.2073	1.2809	14.9840

Å). In other words, the smaller the size of a metal ion, the easier it is expected to diffuse in aqueous systems and the faster is the surface coverage (Horsfall et al. 2006). However, the equilibrium results of the present study revealed that the q_{max} value obtained for Cd^{2+} was greater than that of Pb^{2+}. This, nonetheless, may be explained on the basis of the mechanisms of the adsorption of the three metal ions on SCL. Metal-binding mechanisms include ion-exchange, micro-precipitation, complexation and coordination, which are functions of the functional moieties on the surface of the adsorbent. Therefore, the functional groups on the surface of SCL might have shown different affinities for Cd^{2+}, Pb^{2+} and Zn^{2+} ions (Cazón et al. 2013), as suggested by the FTIR results which reveals weak interaction between –OH and Pb^{2+}. Moreover, although both fit the Langmuir isotherm better than Freundlich, R^2 values (0.986 and 0.969 for Langmuir and Freundlich isotherms, respectively) obtained from the two models for the sorption of Pb^{2+} were closer than those obtained for the sorption of Cd^{2+}, signifying that the adsorption of Pb^{2+} on SCL was both monolayer and multilayer in nature. This possibly suggests that Pb^{2+} was able to access more active sites on SCL, especially in the multilayer region. This assertion was corroborated by time- and concentration-dependence studies (Fig. 6).

The Freundlich intensity constant, n, for the adsorption of the three metals was found to be 2.307, 2.617 and 3.039 for the adsorption of Cd^{2+}, Pb^{2+} and Zn^{2+}, respectively. These values (lying between 0 and 10) indicate that the adsorption of the three metal ions is a physical process. From the Dubinin–Radushkevich model, the mean free energy, E, was found to be 7.207 kJ/mol, 1.281 kJ/mol and 14.984 kJ/mol for Cd^{2+}, Pb^{2+} and Zn^{2+} ions, respectively. The E of adsorption is the free energy change accompanying the transfer of one mole of the metal ion from the bulk solution phase to the surface of the adsorbent (Albadarin et al. 2012). It is expressed as $E=1/\sqrt{2\beta}$. The E values, for Cd^{2+} and Pb^{2+} ions, lie between 1 and 8 kJ/mol, indicating physical adsorption, while the E for Zn^{2+} was found to be between 8 and 16 kJ/mol, suggesting that the ion-exchange mechanism was also involved in the adsorption of Zn^{2+} onto the surface of SCL (Kamal et al. 2010). Table 3 compares the adsorption performance of SCL with other adsorbents. From the values obtained, it can be seen that SCL has a very high efficiency, thereby underscoring its high potential in the removal of toxic divalent heavy metals from polluted water.

Kinetics and mechanism of the process

Two simple kinetic models, Lagergren pseudo-first order and pseudo-second order were applied in explaining the kinetics of the adsorption of Cd^{2+}, Pb^{2+} and Zn^{2+} onto the surface of SCL, while Weber–Morris intra-particle diffusion model was used to explain the mechanism. The linearised forms of the equations are given in Table 1; where q_e (mg/g) and q_t (mg/g) represent the amount of metal adsorbed at equilibrium and time t, respectively; k_1 (min^{-1}) and k_2 (g/mg min) represent pseudo-first-order and pseudo-second-order rate constants, respectively; k_α (mg/g $min^{½}$) represents

Table 3 Comparison of the metal removal efficiency of SCL with other adsorbents

Materials	Experimental conditions			q_m (mg/g)			References
	pH	Temp (°C)	Dose (g)	Cd^{2+}	Pb^{2+}	Zn^{2+}	
Undaria pinnatifida	5.5	25	0.3	–	46.2	–	Zhou et al. (2015)
Coconut shell powder	7	27	5.0	285.7	–	–	Pino et al. (2006)
NaOH-treated rice husk	3.5	25	1.0	–	–	20.08	Muñoz et al. (2018)
Oil palm calyx	5–6	28	0.5	232.558	120.4	–	Oninla et al. (2018)
Cassava tuber bark	5	30	0.005	26.3	–	83.3	Horsfall et al. (2006)
Biomatrix from rice husk	5.5–6	32	3.0	16.7	58.1	8.14	Krishnani et al. (2008)
Treated rubber leaf powder	4	24	0.02	–	95.3	–	Kamal et al. (2010)
Sugarcane leaves	5–6	27	0.1	142.8	156.2	166.7	Present study

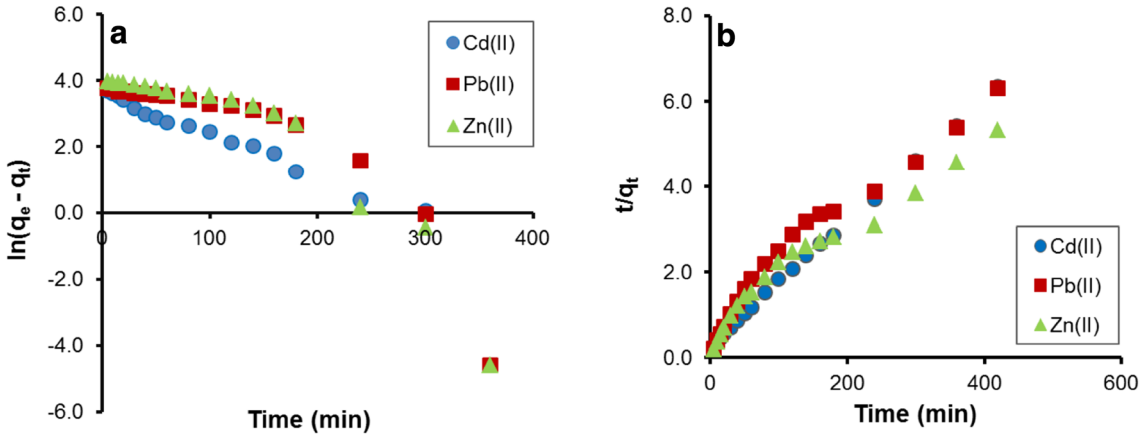

Fig. 7 Pseudo-first-order and pseudo-second-order plots of the adsorption of Cd^{2+}, Pb^{2+} and Zn^{2+} by SCL

intra-particle diffusion rate constant, while *C* represents the intercept. Their linear plots from which parameters were calculated from the slopes and intercepts determined the suitability of the models in explaining the kinetics of the process. Figure 7 depicts the kinetic plots of the models, while Table 2 shows the calculated parameters.

As indicated by the coefficient of determination, R^2, pseudo-second-order model, with R^2 values of 0.999, 0.959 and 0.958 for the adsorption of Cd^{2+}, Pb^{2+} and Zn^{2+}, respectively, better described the kinetics of the adsorption processes than pseudo-first order whose R^2 values are 0.867, 0.763 and 0.829 for Cd^{2+}, Pb^{2+} and Zn^{2+}, respectively. That the data fit the pseudo-second-order model better is an indication that at least two steps were involved in the sorption process: mainly, dissociation of metal/hydronium ions complexes and interaction between metal ions and functional groups present on the adsorbent's surface (Castro et al. 2017). It also suggests the involvement of valency forces, via electron sharing, in the metals/SCL interaction, thus indicating that the biosorption process was controlled by the chemisorption mechanism (Suganya and Kumar 2018). The poorer fittings of the experimental data to pseudo-first order could be due to the general applicability of the model to the initial period during which there is linear increase in sorbate uptake with time (Thitame and Shukla 2016). Weber–Morris intra-particle model indicates that the amount of adsorbate adsorbed is directly proportional to the square root of time. The Weber–Morris equation is given in Table 1. The interpretation of the kinetics of the adsorption process, using this model, is based on the linear plot of q_t versus $t^{1/2}$. If the straight line passes through the origin, intra-particle diffusion is taken as the sole rate-determining step. On the other hand, failure of the line in passing through the origin implies that, at least, one or more of other stages such as external film diffusion, surface diffusion and adsorption at binding sites is/are also involved (Reddy et al. 2011; Suganya and Kumar 2018). The parameters from Weber–Morris plots (Fig. 8) for the adsorption of Cd^{2+}, Pb^{2+} and Zn^{2+} by SCL, presented in Table 2, show that the lines failed to pass through the origin, thus indicating that intra-particle diffusion was not the sole rate-determining step in the removal of Cd^{2+}, Pb^{2+} or Zn^{2+} ions from aqueous solution by SCL. The plots revealed three stages: (a) the initial rapid increase in metal uptake, (b) a linear profile (which indicates gradual increase in metal uptake) and (c) a slow final stage. These three stages have been attributed to the diffusion of the metal ions from the bulk phase en route the SCL interface (external film

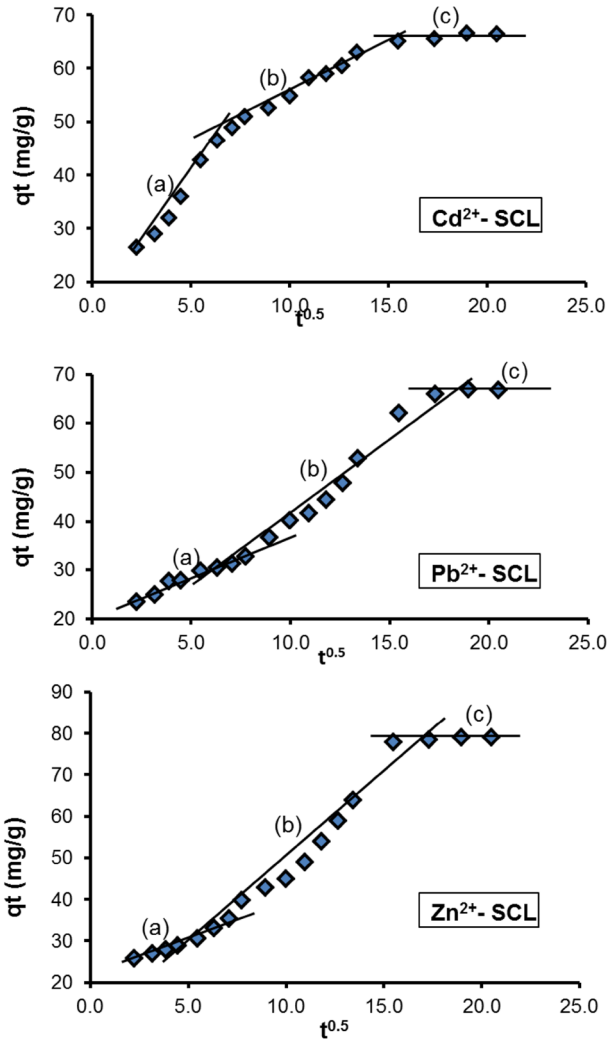

Fig. 8 Weber–Morris model plots of the adsorption of Cd^{2+}, Pb^{2+} and Zn^{2+} by SCL; (a) external film diffusion, (b) intra-particle diffusion, (c) adsorption at the active sites

diffusion), intra-particle diffusion and adsorption at the active sites, respectively (Suganya and Kumar 2018; Thitame and Shukla 2016). High values of the intercepts, 28.8, 14.8 and 13.5, for the adsorption of Cd^{2+}, Pb^{2+} or Zn^{2+} ions by SCL, respectively, suggest that external film diffusion is substantially involved in the sorption process (Thitame and Shukla 2016). Since the adsorption step is known to be fast (Albadarin et al. 2012), the overall rate is generally not affected by it, hence it can be concluded that the two rate-determining steps in the removal of Cd^{2+}, Pb^{2+} or Zn^{2+} ions by SCL were the external film diffusion and the intra-particle diffusion.

Conclusion

SCL, a biomass prepared from an agricultural waste, sugarcane leaves, has been described as an efficient adsorbent in the removal of Cd^{2+}, Pb^{2+} and Zn^{2+} ions. Characterisation of the adsorbent suggested the involvement of the hydroxyl and carboxyl functional groups in the binding of the metal ions. The surface of the adsorbent was composed of scattered pores with altered morphology after metal uptake. Carbon and oxygen were the dominant elements present in the biomass and their abundant presence ensured the availability of the functional moieties involved in the metal-binding process. Quantitatively, pH had a significant influence on the amount of metal ions removed. The kinetics of the removal of Cd^{2+}, Zn^{2+} and Pb^{2+} was observed to be relatively fast, especially at the first stage of the adsorption process. As high as 250 mg/L metal ion concentration was effectively removed by as low as 50 mg SCL, underscoring the high potentials of the adsorbent in heavy metal removal. Equilibrium data fit Langmuir isotherm better than Freundlich and D–R isotherms, indicating monolayer adsorption and independent occupation of the active sites by the metal ions. The maximum metal uptake, q_e, values calculated for the removal the three metals underline the high efficiency and effectiveness of SCL in the removal of toxic metal ions. Information from the Freundlich and D–R isotherms attributes the removal of Cd^{2+}, Pb^{2+} and Zn^{2+} to physisorption, with ion-exchange mechanism involved in Zn^{2+} adsorption as well. Kinetic data from the sorption of the three metal ions fit the pseudo-second-order model better than pseudo-first order, suggesting chemisorption as the rate-determining step in the biosorption mechanism. The Weber–Morris model indicates that the intra-particle diffusion and external film diffusion are the two rate-determining steps.

Acknowledgements The authors acknowledge the Department of Chemistry, University of Ibadan, where the major part of the work was carried out; as well as the Polymer and Biophysical Chemistry Research Laboratory, Obafemi Awolowo University, Ile-Ife and the Central Research Laboratory, University of Ibadan, Nigeria.

References

Albadarin, A. B., Mangwandi, C., Al-Muhtaseb, A. H., Walker, G. M., Allen, S. J., & Ahmad, M. N. M. (2012). Kinetic and thermodynamics of chromium ions adsorption onto low-cost dolomite adsorbent. *Chemical Engineering Journal, 179,* 193–202.

AOAC. (1990). *Official methods of Analysis* (15th ed.). Virginia, USA: Association of Official Analytical Chemist Inc.

Babalola, J. O., Koiki, B. A., Eniayewu, Y., Salimonu, A., Olowoyo, J. O., Oninla, V. O., et al. (2016). Adsorption efficacy of *Cedrela odorata* seed waste for dyes: Non linear fractal kinetics and non linear equilibrium studies. *Journal of Environmental Chemical Engineering, 4,* 3527–3536.

Castro, L., Blázquez, M. L., González, F., Muñoz, J. A., & Ballester, A. (2017). Biosorption of Zn(II) from industrial effluents using sugar beet pulp and *F. vesiculosus*: From laboratory tests to a pilot approach. *Science of the Total Environment, 598,* 856–866.

Cazón, J. P., Viera, M., Donati, E., & Guibal, E. (2013). Zinc and cadmium removal by biosorption on *Undaria pinnatifida* in batch and continuous processes. *Journal of Environmental Management, 129,* 423–434.

Cotton, F. A., & Wilkinson, G. (1980). *Advanced inorganic chemistry—a comprehensive text* (4th ed.). New York: Wiley.

Denny, P. (1997). Implementation of constructed wetlands in developing countries. *Water Science and Technology, 35,* 27–34.

Dubinin, M. M., Zaverina, E. D., & Radushkevich, L. V. (1947). Sorption and structure of active carbons. I. Adsorption of organic vapors. *Zhurnal Fizicheskoi Khimii, 21,* 1351–1362.

Freundlich, H. M. F. (1906). Uber die adsorption in lasungen. *Zeitschrift für Physikalische Chemie, 57,* 385–470.

Gnanasekaran, L., Hemamalini, R., & Ravichandran, K. (2015). Synthesis and characterization of TiO_2 quantum dots for photocatalytic application. *Journal of Saudi Chemical Society, 19,* 589–594.

Hassoune, J., Tahiri, S., El Krati, M., Cervera, M. L., & de la Guardia, M. (2018). Removal of hexavalent chromium from aqueous solutions using biopolymers. *Journal of Environmental Engineering*. https://doi.org/10.1061/(asce)ee.1943-7870.0001396.

Ho, Y. S., & McKay, G. (1999). Pseudo-second order model for sorption processes. *Process Biochemistry, 34,* 451–465.

Horsfall, M., Jr., Abia, A. A., & Spiff, A. I. (2006). Kinetic studies on the adsorption of Cd^{2+}, Cu^{2+} and Zn^{2+} ions from aqueous solutions by cassava (*Manihot esculenta Cranz*) tuber bark waste. *Bioresource Technology, 97,* 283–291.

Jin, Y., Teng, C., Yu, S., Song, T., Dong, L., Liang, J., et al. (2018). Batch and fixed-bed biosorption of Cd(II) from aqueous solution using immobilized *Pleurotus ostreatus* spent substrate. *Chemosphere, 191,* 799–808.

Kamal, M. H. M. A., Azira, W. M. K. W. K., Kasmawati, M., Haslizaidi, Z., & Saime, W. W. (2010). Sequestration of toxic Pb(II) ions by chemically treated rubber (*Hevea brasiliensis*) leaf powder. *Journal of Environmental Sciences, 22,* 248–256.

Krishnani, K. K., Meng, X., Christodoulatos, C., & Boddu, V. M. (2008). Biosorption mechanism of nine different heavy metals onto biomatrix from rice husk. *Journal of Hazardous Materials, 153,* 1222–1234.

Lagergren, S. (1898). About the theory of so-called adsorption of soluble substances. *Kungliga Svenska Vetenskapsakademiens Handlingar Band, 124,* 1–39.

Langmuir, I. (1918). The adsorption of gases on plane surfaces of glass, mica and platinum. *Journal of the American Chemical Society, 40,* 1361–1402.

Liu, J., Liu, X., Sun, Y., Sun, C., Liu, H., Stevens, L. A., et al. (2018). High density and super ultra-microporous-activated carbon macrospheres with high volumetric capacity for CO_2 capture. *Advanced Sustainable Systems, 2*(2), 1700115. https://doi.org/10.1002/adsu.201700115.

Muñoz, A. J., Espínola, F., & Ruiz, E. (2018). Removal of heavy metals by *Klebsiella* sp. 3S1. Kinetics, equilibrium and interaction mechanisms of Zn(II) biosorption. *Journal of Chemical Technology and Biotechnology, 93,* 1370–1380.

Naushad, M., Ahamad, T., Sharma, G., Ai-Muhtaseb, A. H., Albadarin, A. B., Alam, M. M., et al. (2016). Synthesis and characterization of a new starch/SnO2 nanocomposite for efficient adsorption of toxic Hg^{2+} metal ion. *Chemical Engineering Journal, 300,* 306–316.

Ofomaja, A. E., & Naidoo, E. B. (2011). Biosorption of copper from aqueous solution by chemically activated pine cone: A kinetic study. *Chemical Engineering Journal, 175,* 260–270.

Oninla, V. O., Olatunde, A. M., Babalola, J. O., Adesanmi, O. J., Towolawi, G. S., & Awokoya, K. N. (2018). Qualitative assessments of the biomass from oil palm calyxes and its application in heavy metals removal from polluted fresh water. *Journal of Environmental Chemical Engineering, 6,* 4044–4053.

Pino, G. H., de Mesquita, L. M. S., Torem, M. L., & Pinto, G. A. S. (2006). Biosorption of cadmium by green coconut shell powder. *Minerals Engineering, 19,* 380–387.

Qin, Y., Liu, C., Jiang, S., Xiong, L., & Sun, Q. (2016). Characterization of starch nanoparticles prepared by nanoprecipitation: Influence of amylose content and starch type. *Industrial Crops and Products, 87,* 182–190.

Reddy, D. K. V., Seshaiah, R. K., & Reddy, A. V. R. (2011). Biosorption of Ni(II) from aqueous phase by *Moringa oleifera* bark, a low cost biosorbent. *Desalination, 268,* 150–157.

Suganya, S., & Kumar, P. S. (2018). Influence of ultrasonic waves on preparation of active carbon from coffee waste for the reclamation of effluents containing Cr(VI) ions. *Journal of Industrial and Engineering Chemistry, 60,* 418–430.

Thitame, P. V., & Shukla, S. R. (2016). Adsorptive removal of reactive dyes from aqueous solution using activated carbon synthesized from waste biomass materials. *International Journal of Environmental Science and Technology, 13,* 561–570.

Vijayaraghavan, K., Rangabhashiyam, S., Ashokkumar, T., & Arockiaraj, J. (2017). Assessment of samarium biosorption from aqueous solution by brown macroalga *Turbinaria conoides*. *Journal of the Taiwan Institute of Chemical Engineers, 74,* 113–120.

Weber, W. J., & Morris, J. S. (1963). Kinetics of adsorption on carbon from solution. *Journal of the Sanitary Engineering Division, 89,* 31–59.

Zhou, K., Yang, Z., Liu, Y., & Kong, X. (2015). Kinetics and equilibrium studies on biosorption of Pb(II) from aqueous solution by a novel biosorbent: *Cyclosorus interruptus*. *Journal of Environmental Chemical Engineering, 3,* 2219–2228.